Kinetics and Catalysis, Vol. 45, No. 5, 2004, pp. 702–707. Translated from Kinetika i Kataliz, Vol. 45, No. 5, 2004, pp. 742–747.

Formation of the Pore Structure of Oxide Vanadium–Titanium–Phosphorus Catalysts in the Course of Thermal Treatment

V. Yu. Gavrilov, G. A. Zenkovets, O. V. Zalomaeva, and S. V. Tsybulya

Boreskov Institute of Catalysis, Siberian Division, Russian Academy of Sciences, Novosibirsk, 630090 Russia

Received March 28, 2003

Abstract—The effect of the conditions of the thermal treatment of vanadium–titanium–phosphorus catalysts on the formation of the pore structure and phase composition was studied. It was found that the optimum doping of catalysts with phosphorus (5 wt % P_2O_5) was favorable for retention of the high dispersity of primary particles up to 450°C. The main change in the texture of the catalysts occurred within the range of micropores and mesopores with $D < 10$ nm. The formation of the coarsely dispersed well-crystallized phase of a vanadium–titanium–phosphorus compound was detected.

INTRODUCTION

Vanadium–titanium oxide catalysts modified with molybdenum, tungsten, and phosphorus are used in a number of important industrial partial oxidation processes. Vanadium–titanium catalysts containing phosphorus additives are active and selective in reactions such as the oxidation of *ortho*-xylene [1], toluene [2, 3], and butadiene [4]; the oxidative ammonolysis of methylpyrazine [5]; the reduction of nitrogen oxides with ammonia in the presence of sulfur compounds [6] and oxygen [7]; the oxidative dehydrogenation of ethane to ethylene [8]; and the oxidation of *n*-butane to maleic anhydride [9].

In the development of new oxide catalysts, it is important to study the formation of the pore structure and the dispersity of components along with the phase composition and other physicochemical properties, because the stability of the structure parameters of catalysts under reaction conditions has a determining effect on performance characteristics.

The temperature conditions of treatment are an important factor affecting the texture parameters and phase composition of catalysts. Moreover, the introduction of various additives also exerts a considerable effect on the thermal stability of oxide catalysts. In this case, the chemical nature and concentration of an additive are important. As was found previously [10, 11], vanadium or molybdenum additives to titanium dioxide significantly increase the thermal stability in comparison with the initial support [12]. At the same time, the simultaneous doping of titanium dioxide with molybdenum and vanadium results in a dramatic decrease in the thermal stability of the catalyst [11].

Published data on the effect of phosphorus additives on the formation of the texture of vanadium–titanium catalyst are scanty; as a rule, these data are unsystematic and discrepant. At the same time, it was reliably found that these additives are an effective factor for changing the strength characteristics of molded catalysts [13].

The aim of this work is to examine the effects of the conditions of thermal treatment and the composition of oxide vanadium–titanium–phosphorus (V–Ti–P) catalysts on the formation of the dispersity of components and on the pore structure.

EXPERIMENTAL

The oxide V–Ti–P catalysts with the composition 1–15 wt % P_2O_5, 20 wt % V_2O_5, and 79–65 wt % TiO_2 were synthesized by mixing titanium hydroxide in the anatase modification, which was prepared by the industrial sulfuric acid technology [14], with vanadyl oxalate and phosphoric acid solutions followed by drying in an Anhydro spray drier. The resulting powder was pelletized, and the pellets were subjected to thermal treatment at 300–550°C in a flow of air for 4 h. No changes in the chemical composition of the catalysts as a result of the volatility of the components were observed in the course of high-temperature treatment.

The pore structure of the prepared catalysts was studied by low-temperature (77.4 K) adsorption of nitrogen with a DigiSorb-2600 Micrometrics instrument. The true density ρ (g/cm^3) was measured with an AutoPycnometer-1320 Micrometrics instrument using helium. The total pore volume V_Σ (cm^3/g) and the porosity ε (cm^3/cm^3) were calculated from the bulk density δ (g/cm^3) and the true density using the well-known relationships $V_\Sigma = (0.6\delta^{-1} - \rho^{-1})$ and $\varepsilon = V_\Sigma\rho(1 + V_\Sigma\rho)^{-1}$. The limiting sorption-space volume V_s (cm^3/g), that is, the micropore and mesopore part of the pore space, was determined directly from adsorption experiments. The mesopore and macropore surface area

0023-1584/04/4505-0702 © 2004 MAIK "Nauka/Interperiodica"

Table 1. X-ray diffraction data for oxide V–Ti–P catalysts treated at various temperatures

Sample	*T*, °C		
	300, 350, 400, 450	500	550
1% P_2O_5 : 20% V_2O_5 : 79% TiO_2	Anatase, rutile, and V_2O_5	Anatase, rutile, and V_2O_5	Anatase, rutile, and V_2O_5
3% P_2O_5 : 20% V_2O_5 : 77% TiO_2	″	″	″
5% P_2O_5 : 20% V_2O_5 : 75% TiO_2	″	″	Anatase, rutile, V_2O_5, and X
10% P_2O_5 : 20% V_2O_5 : 70% TiO_2	Anatase, rutile	Anatase, rutile, V_2O_5, and X	″
15% P_2O_5 : 20% V_2O_5 : 65% TiO_2	″	″	″

S_α(m^2/g) and the micropore volume V_μ (cm^3/g) were determined by a comparative method of treating N_2 adsorption isotherms in accordance with a published procedure [15]. The average size d (nm) of the primary catalyst particles was estimated by the relation $d = 6S^{-1}\rho^{-1}$. The pore size distribution according to the equivalent sizes of pore entrances was calculated from the desorption branches of nitrogen adsorption isotherms using the classical Barrett–Joyner–Halenda method [16].

The X-ray diffraction analysis of the samples was performed on a URD-63 diffractometer with monochromatic CuK_α radiation. The sizes of the coherent-scattering regions (CSRs) of anatase particles and vanadium pentoxide were traditionally determined by the Scherrer formula [17] using the halfwidths of the 2.0.0. and 4.0.0. diffraction peaks, respectively.

RESULTS AND DISCUSSION

Table 1 summarizes the data on the X-ray diffraction analysis of catalysts treated at various temperatures. A small amount of rutile (~5–10 wt %) occurred in the parent titanium dioxide. In the samples with 1–3 wt % P_2O_5, the fraction of rutile (relative to anatase) remained unchanged up to 500°C; simultaneously, a V_2O_5 phase with a CSR of about 20 nm was detected. After calcination at 550°C, the amount of rutile increased insignificantly. The rutile content of the sample containing 5 wt % P_2O_5 dramatically increased after heating at 550°C, and lines due to a new phase (denoted by X in Table 1) with interplanar spacings of 3.35, 3.67, and 4.12 Å appeared (Fig. 1). In the samples with higher phosphorus contents (10–15 wt % P_2O_5), only a mixture of anatase and rutile was detected in the temperature range 300–450°C. After calcination at 500°C or higher, anatase, rutile, and V_2O_5 phases and the well-crystallized phase X were detected (Fig. 2). In this case, the fractions of rutile and the crystallized phase X increased with temperature. Simultaneously, the CSR of the phase X also increased, from 15–18 nm at 500°C to 22–28 nm at 550°C. It is likely that the absence of a V_2O_5 phase detected at a temperature lower than 500°C was due to the formation of an initially amorphous vanadium–titanium–phosphorus compound. In this case, a lower P_2O_5 content (1–5 wt %) did not result in the complete binding of vanadium pentoxide.

Table 2 summarizes the experimental data obtained by adsorption techniques and calculated from bulk and

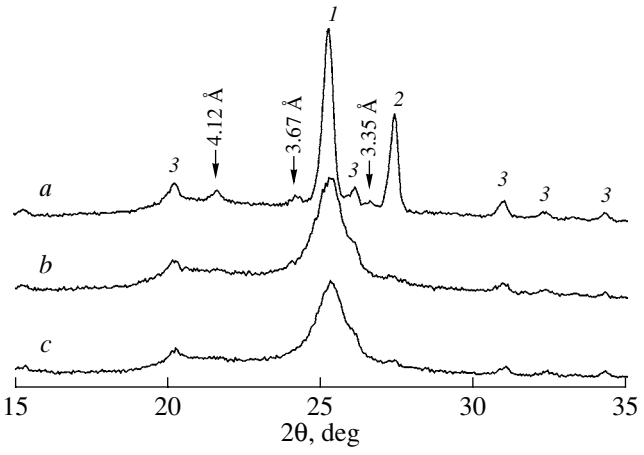

Fig. 1. X-ray diffraction patterns of samples containing 5 wt % P_2O_5 calcined at (*a*) 300, (*b*) 400, and (*c*) 550°C. Characteristic peaks: (*1*) anatase, (*2*) rutile, and (*3*) V_2O_5. Arrows indicate the peaks of phase X.

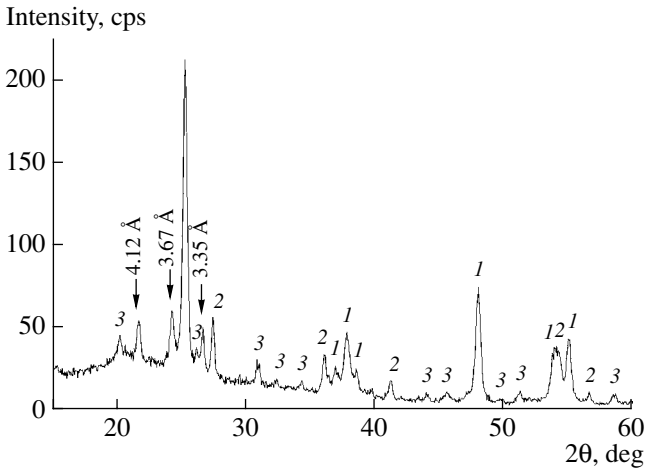

Fig. 2. X-ray diffraction pattern of a sample containing 15 wt % P_2O_5 calcined at 500°C. Characteristic peaks: (*1*) anatase, (*2*) rutile, and (*3*) V_2O_5. Arrows indicate the peaks of phase X.

Table 2. Texture parameters of the oxide V–Ti–P catalysts treated at various temperatures

Sample	T, °C	ρ, g/cm^3	V_s, cm^3/g	V_μ, cm^3/g	S_α, m^2/g	d, nm	δ, g/cm^3	V_Σ, cm^3/g	β	ε, cm^3/cm^3	D_{CSR}, nm
1% P_2O_5 : 20% V_2O_5 : 79% TiO_2	300	–	0.253	0.019	128	–	0.73	–	–	–	7
	350	3.34	0.228	0.003	149	12	0.74	0.51	0.45	0.63	8.5
	400	3.36	0.269	0	108	15	0.77	0.48	0.56	0.62	8.5
	450	3.39	0.283	0	95	20	0.75	0.51	0.55	0.63	12
	500	3.40	0.192	0	24	75	0.74	0.52	0.37	0.64	19
	550	3.47	0.202	0	22	80	0.75	0.51	0.39	0.64	23
3% P_2O_5 : 20% V_2O_5 : 77% TiO_2	300	3.31	0.214	0.013	133	15	0.72	0.53	0.40	0.64	6
	350	3.35	0.203	0.005	129	15	–	–	–	–	7
	400	3.46	0.226	0.009	117	15	–	–	–	–	7.5
	450	3.52	0.222	0	85	20	0.68	0.60	0.36	0.68	15
	500	3.64	0.222	0	19	90	0.66	0.63	0.35	0.70	22
	550	3.78	0.204	0	22	70	0.68	0.62	0.33	0.70	23
5% P_2O_5 : 20% V_2O_5 : 75% TiO_2	300	3.14	0.235	0.021	110	15	0.72	0.51	0.46	0.62	7
	350	3.18	0.249	0.019	121	15	0.73	0.51	0.49	0.62	7.5
	400	3.22	0.238	0.005	119	15	0.76	0.48	0.50	0.61	7
	450	3.52	0.275	0.004	116	15	0.75	0.52	0.53	0.64	8
	500	3.70	0.265	0	78	20	0.72	0.56	0.47	0.68	15
	550	3.82	0.216	0	21	75	0.73	0.56	0.39	0.68	29
10% P_2O_5 : 20% V_2O_5 : 70% TiO_2	300	–	0.146	0.014	69	–	0.75	–	–	–	7
	400	3.30	0.135	0.002	38	50	0.70	0.55	0.25	0.65	7.5
	450	3.44	0.171	0.001	41	45	0.71	0.55	0.31	0.66	18
	500	3.65	0.143	0	15	110	0.69	0.60	0.24	0.68	19
	550	3.66	0.123	0	10	160	0.66	0.64	0.19	0.69	29
15% P_2O_5 : 20% V_2O_5 : 65% TiO_2	300	3.16	0.095	0	19	100	0.63	0.64	0.15	0.67	8
	350	3.11	0.106	0	20	95	0.65	0.60	0.18	0.65	7.5
	400	3.27	0.115	0	20	90	0.71	0.54	0.21	0.64	8
	450	3.30	0.135	0	21	85	0.67	0.58	0.23	0.65	10
	500	3.68	0.149	0	18	90	0.77	0.51	0.29	0.65	18
	550	3.60	0.099	0	10	160	0.73	0.54	0.18	0.66	29

true densities. It can be seen that the texture parameters of catalysts depend on the chemical composition and the conditions of thermal treatment. In all the samples, the true density ρ monotonically increased with calcination temperature, whereas its dependence on the chemical composition was more complex. It can be seen that the values of ρ for the majority of catalysts were lower than the density of the main component, which was pure anatase (3.84 g/cm^3). As a rule, this is a sign of the occurrence of a detectable amount of the amorphous phase of titanium dioxide, the crystallization of which in the course of thermal treatment is responsible for the main increase in the true density.

It can also be seen in Table 2 that the vanadium–titanium–phosphorus catalysts have a noticeable micropore volume V_μ, which depends considerably on the phosphorus content and on calcination temperature. Thus, in the sample containing 1 wt % P_2O_5, micropores were detected at temperatures of up to 350°C. In the sample with 5 wt % P_2O_5, micropores with a noticeable volume were observed at temperatures of up to 450°C; however, the micropore volume decreased as the phosphorus content was further increased. Previously [12], it was found that micropores were related to titanium dioxide used in the synthesis of catalysts, which was obtained by the hydrolysis of titanium sulfate salts. The residual products of the incomplete hydrolysis of a precursor resulted in the formation of micropores in the xerogel. The further fate of micropores in the course of thermal treatment depended on the chemical composition of the catalyst. In pure TiO_2, micropores disappeared even at 300°C; the doping of titanium dioxide with molybde-

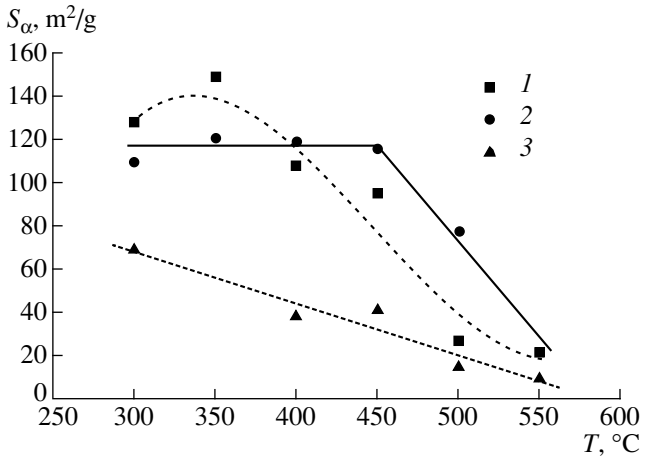

Fig. 3. Dependence of the value of S_α of phosphorus–vanadium–titanium catalysts on the temperature of treatment: (*1*) 1, (*2*) 5, and (*3*) 10 wt % P_2O_5.

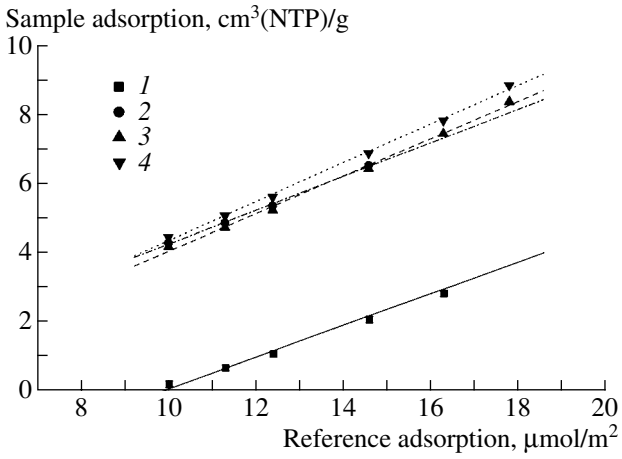

Fig. 4. Nitrogen adsorption isotherms (on the coordinates of a comparative method) on the catalyst containing 15% P_2O_5, 20% V_2O_5, and 65% TiO_2 calcined at T, °C: (*1*) 300, (*2*) 350, (*3*) 400, and (*4*) 450.

num facilitated the retention of micropores at temperatures of up to 400°C [11].

Figure 3 demonstrates the curves of changes in the surface areas of mesopores and macropores (S_α) in oxide V–Ti–P catalysts in the course of thermal treatment. It can be seen that the thermal stability of the samples, that is, the ability to retain a high average dispersity d of primary particles, was different, and it depended on the composition of the catalyst. In catalysts containing 1 wt % P_2O_5, an increase in S_α was initially observed (at 300–350°C), which then changed to a dramatic decrease. This behavior of the experimental dependence was due to the disappearance (consolidation) of micropores and the corresponding formation of an additional volume of fine mesopores. As mentioned above, the occurrence of a micropore part of the texture in all of the other catalysts was observed up to high treatment temperatures, when the consolidation of micropores and the agglomeration of primary catalyst particles occurred simultaneously because of surface sticking and, partially, a phase transition. As a result, the mesopore and macropore surface area of the catalyst containing 5 wt % P_2O_5, 20 wt % V_2O_5, and 75 wt % TiO_2 remained practically constant up to 450°C and decreased only at higher temperatures. A further increase in the phosphorus content of the catalyst, up to 10–15 wt % P_2O_5, facilitated the agglomeration of primary particles, a considerable decrease in the mesopore volume, and, as a result, a dramatic decrease in the surface area of mesopores and macropores.

Figure 4 exemplifies the comparative plots of the adsorption isotherms of nitrogen on the catalyst containing 15 wt % P_2O_5. The experimental data on nitrogen adsorption on oxide surfaces, published by Gregg and Sing [16], were used as reference adsorption. Note that the extremely weak sorption of nitrogen at low sorbate pressures was observed in the sample calcined at 300°C, in contrast to the other isotherms of this and the other catalysts. This manifested itself in the concave shape of the initial portion of the isotherm and in the greater negative intercept on the axis of ordinates of the comparative plot (Fig. 4). It is well known that a decrease in the energy of adsorption is primarily responsible for weakening the sorption of nitrogen molecules on a solid surface [15]. It is believed that this feature of the sorption process is due to the presence of molecular-size fragments on the surface of a catalyst. This results in a weakening of the cooperative dispersion interaction of nitrogen molecules with the surface atoms of the catalyst and, consequently, in a loosening of the first adsorption layer; however, the structure of the next layer remains almost unaffected [15, 18]. It is likely that these fragments became consolidated as the treatment temperature was increased to 350°C, and the dispersion interaction in the first adsorption layer recovered largely. It is also believed that the nature of these molecular fragments on the surface is related to the presence of phosphorus in considerable amounts in the catalyst.

Table 2 also summarizes the values of $\beta = V_s/V_\Sigma$, the fraction of micropores and mesopores in the total pore volume of catalysts. It can be seen that, as a rule, the value of β does not considerably exceed 0.5; that is, macropores, which cannot be analyzed by adsorption techniques, are responsible for a considerable portion of the pore space. The value of β passed through a maximum as the temperature of sample treatment was increased. In this case, an increase in the phosphorus content above 5 wt % P_2O_5 resulted in a decrease in the value of β. Note that the position of the maximum of β was shifted toward the region of higher temperatures as the phosphorus content of the catalyst was increased, with a simultaneous decrease in the value of β. At the same time, the catalyst porosity ε did not exhibit con-

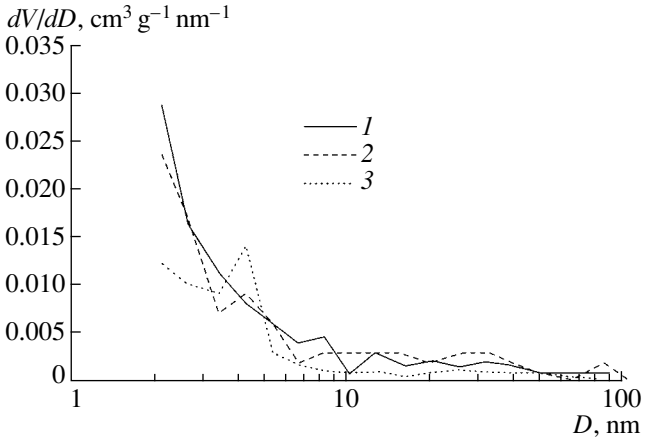

Fig. 5. Differential curves of pore-volume distribution according to the size for the samples calcined at 300°C: (*1*) 1, (*2*) 5, and (*3*) 10 wt % P_2O_5.

siderable change; this fact suggests the absence of deep bulk agglomeration processes. Consequently, it is believed that changes in the texture of the catalysts over the test temperature range primarily occurred in the range of micropores and the finest mesopores, the fraction of which in the total pore volume is small.

Figures 5 and 6 demonstrate the differential curves of mesopore-volume distribution according to the equivalent size of pore entrances for catalysts calcined at 300 and 450°C. In can be seen that, at a minimum temperature of calcination, the catalysts with phosphorus concentrations of 1–5 wt % P_2O_5 were approximately identical, and a noticeable decrease in the volumes of the finest mesopores with $D < 3$ nm was observed only at a higher concentration of phosphorus. At the same time, the texture of all the catalysis in the range of pores with $D > 10$ nm was approximately the same. An increase in the phosphorus content and in the temperature of treatment (Fig. 6) resulted in a dramatic decrease in the volume of pores with $D < 10$ nm for the catalyst with 10 wt % P_2O_5, whereas the greatest volumes of fine pores were retained in the sample with 5 wt % P_2O_5; this provided the retention of the greatest surface area S_α in this catalyst.

Figure 7 demonstrates the differential curves of mesopore-volume distribution for the most thermally stable catalyst containing 5 wt % P_2O_5, 20 wt % V_2O_5, and 75 wt % TiO_2. It follows from Fig. 7 that a noticeable decrease in the volume of the finest mesopores with $D < 3$ nm occurred only at 500°C, whereas the distribution of mesopores with $D > 8$ nm remained practically unchanged. This fact provides support for the hypothesis that only the texture of micropores and mesopores with $D < 8$–10 nm changed over the test temperature range. The fraction of these pores in the total pore volume of the catalysts is small and equal to ~0.08–0.10 (the volume of fine mesopores was estimated from the differential curve of pore-size distribution). The transformation of the texture in only an insignificant part of the pore space explains the absence of a stable trend of changes in the total porosity of the catalysts.

A comparison of the data on the average particle size d of a catalyst and on the CSRs of anatase particles (Table 2) allowed us to state that, to a first approximation, the CSR size is independent of catalyst composition and depends only on the temperature of treatment, whereas the value of d depends on both catalyst composition and temperature.

The initial interaction of the components and the appearance of the phases of an oxide vanadium–titanium–phosphorus catalyst occurred at the stage of the spray drying of the parent suspensions. Highly dispersed anatase particles, an amount of rutile and amorphous titania, and the amorphous phase of a vanadium–titanium–phosphorus compound were formed in this process. At a low phosphorus content (1–5 wt % P_2O_5), an excess amount of vanadium pentoxide was retained,

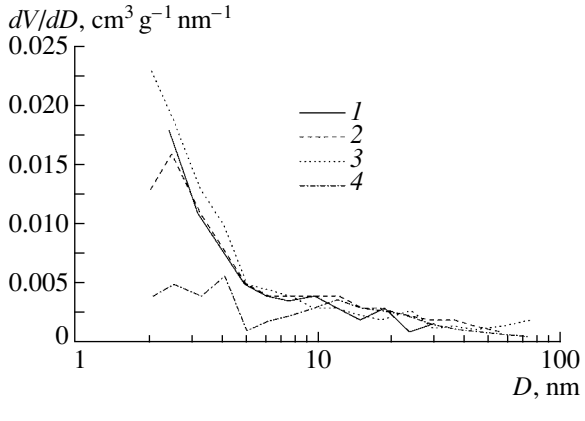

Fig. 6. Differential curves of pore-volume distribution according to the size for the samples calcined at 450°C and containing (*1*) 1, (*2*) 3, (*3*) 5, and (*4*) 10 wt % P_2O_5.

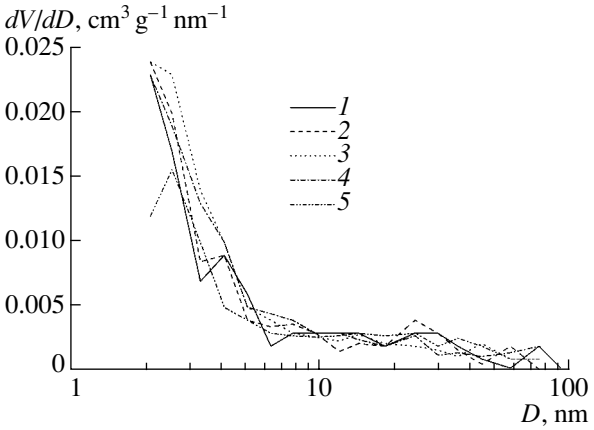

Fig. 7. Differential curves of pore-volume distribution according to the size for the sample containing 5 wt % P_2O_5 calcined at (*1*) 300, (*2*) 350, (*3*) 400, (*4*) 450, and (*5*) 500°C.

which was detected by X-ray diffraction analysis (Table 1). An increase in the amount of added phosphorus, to 10–15 wt % P_2O_5, resulted in the complete binding of vanadium in an initially amorphous vanadium–titanium–phosphorus compound. As noted above, as the treatment temperature was increased above 500°C, this compound transformed into a well-crystallized phase X and superstoichiometric vanadium pentoxide released. A detailed study of the structure and chemical composition of the phase X will be the subject matter of subsequent publications.

The experimental data suggest that an optimum amount of the amorphous vanadium–titanium–phosphorus compound (in the catalyst containing 5 wt % P_2O_5) provides the highest thermal stability of the catalyst, that is, the retention of a high average dispersity of particles. It is believed that an increase in the thermal stability of the catalyst is related to sufficient stability of the phase of the V–Ti–P compound; in turn, this prevents dispersed components from agglomerating. At the same time, a deviation from the optimum amount (1–3 or 10–15 wt % P_2O_5), on the one hand, precludes the stabilization of the total pore space of the catalyst and, on the other hand, results in the filling of the finest pores (Fig. 6) with a simultaneous decrease in the specific surface area and an increase in the average calculated catalyst particle size *d*.

REFERENCES

1. Hengstum, A.J., Pranger, J., Ommet, J.G., and Gellings, P.J., *Appl. Catal.*, 1984, vol. 11, no. 3, p. 317.
2. Zhu, J., Robenstorf, B., and Andersson, S.L.T., *J. Chem. Soc., Faraday Trans. I.*, 1989, vol. 85, no. 11, p. 3645.
3. Bond, G.C. and Tahir, S.F., *Catal. Today.*, 1991, vol. 10, no. 3, p. 393.
4. Deo, G. and Wachs, I.E., *J. Catal.*, 1994, vol. 146, no. 2, p. 335.
5. Bondareva, V.M., Andrushkevich, T.V., and Zenkovets, G.A., *The Second Int. Boreskov Memorial Conference "Catalysis on the Eve of the XXI Century,"* Novosibirsk, 1997, part 2, p. 164.
6. Busca, G., Lietti, L., Ramis, G., and Berti, F., *Appl. Catal., B.*, 1998, vol. 18, no. 1, p. 1.
7. Blanco, J., Avila, P., Barthelemy, C., and Valdenebro, A.G., *Appl. Catal.,* 1990, vol. 63, no. 2, p. 403.
8. El-Drissi, J., Kacimi, M., Loukah, M., and Ziyad, M., *J. Chim. Phys. Phys.-Chim. Biol.*, 1997, vol. 94, nos. 11–12, p. 1984.
9. Guliants, V.V., Benziger, J.B., Sundaresan, S., Wachs, I.E., and Hirt, A.M., *Catal. Lett.*, 1999, vol. 62, nos. 2–4, p. 87.
10. Zenkovets, G.A., Gavrilov, V.Yu., Kryukova, G.N., and Tsybulya, S.V., *Kinet. Katal.*, 1998, vol. 39, no. 1, p. 122.
11. Zenkovets, G.A., Gavrilov, V.Yu., Kryukova, G.N., Tsybulya, S.V., and Parmon, V.N., *Kinet. Katal.*, 2002, vol. 43, no. 4, p. 621.
12. Gavrilov, V.Yu. and Zenkovets, G.A., *Kinet. Katal.*, 1993, vol. 34, no. 2, p. 357.
13. Blanco, J., Avila, P., Barthelemy, C., Bahamonde, A., Odriozola, J.A., Garcia DeLa Banda, J.F., and Heinemann, H., *Appl. Catal.*, 1989, vol. 55, no. 1, p. 151.
14. Dolmatov, Yu.D. and Sheikman, A.I., *Zh. Prikl. Khim.*, 1970, vol. 43, no. 2, p. 249.
15. Karnaukhov, A.P., *Adsorbtsiya. Tekstura dispersnykh i poristykh materialov* (Adsorption: Texture of Dispersed and Porous Materials), Novosibirsk: Nauka, 1999.
16. Gregg, S.J. and Sing, K.S.W. *Adsorption, Surface Area and Porosity*, London: Academic, 1982.
17. Gin'e, A., *Rentgenografiya kristallov. Teoriya i praktika* (X-ray Crystal Structure: Theory and Practice), Moscow: Fizmatgiz, 1961.
18. Gavrilov, V.Yu., Zagrafskaya, R.V., Karnaukhov, A.P., and Fenelonov, V.B., *Kinet. Katal.*, 1981, vol. 22, no. 2, p. 452.